

## Soft x-ray magnetic circular dichroism investigation of the spin reorientation transition in Nd<sub>2</sub>Fe<sub>14</sub>B

L. M. García,<sup>a)</sup> J. Chaboy, and F. Bartolomé

*Instituto de Ciencia de Materiales de Aragón, CSIC-Universidad de Zaragoza, Facultad de Ciencias, E. 50009, Zaragoza, Spain*

J. B. Goedkoop

*Faculty of Mathematics, Computer Science, Physics and Astronomy, University of Amsterdam, The Netherlands*

A temperature dependent x-ray magnetic circular dichroism (XMCD) study at the Fe  $L_{2,3}$  and Nd  $M_{4,5}$  edges through the spin reorientation transition of a Nd<sub>2</sub>Fe<sub>14</sub>B single crystal is presented. Direct comparison of XMCD data with values of the magnetic moments derived from Mössbauer spectroscopy allows one to independently determine the evolution of the tilting angle between Fe and Nd moments and the  $c$  axis. The experimental results evidence a strong noncollinearity between Fe and Nd magnetic moments in the low-temperature phase. A new result is the observed delay in the reorientation of the Fe sublattice with respect to that of the Nd sublattice by around 10 K.

© 2000 American Institute of Physics. [S0021-8979(00)91308-2]

Since the discovery in the 1980s of the R<sub>2</sub>Fe<sub>14</sub>B intermetallic compounds,<sup>1,2</sup> Nd<sub>2</sub>Fe<sub>14</sub>B has become the highest performance permanent magnet material. Because of the huge high-tech market in which permanent magnets are used, much research has been focused on Nd<sub>2</sub>Fe<sub>14</sub>B in order to understand its complex magnetic behavior.<sup>3</sup> Nd<sub>2</sub>Fe<sub>14</sub>B has a tetragonal crystal structure belonging to the space group  $P4_2/mnm$  and showing six nonequivalent sites for iron and two for neodymium. At room temperature, the magnetic anisotropy is uniaxial; both Fe and Nd magnetic moments are parallel oriented along the [001] direction ( $c$  axis). By decreasing temperature, a spin reorientation transition (SRT) takes place at  $T_{\text{SRT}} \sim 135$  K.<sup>4</sup> Below  $T_{\text{SRT}}$  magnetization begins to deviate from the  $c$  axis toward the [110] axis, reaching a tilting angle with the  $c$  axis of 30.6° at 4.2 K.<sup>5</sup> The magnetic structure of Nd<sub>2</sub>Fe<sub>14</sub>B below the SRT has been a subject of controversy in the last several years. In particular, the question which arises is whether or not there is a canting of the Nd and Fe spins relative to one another or whether they remain basically collinear as in the high temperature phase.<sup>3</sup>

Theoretical calculations based on magnetization analysis predict that the Nd moments are 2°–3° collinear with the Fe sublattice magnetization in the low-temperature phase.<sup>6</sup> On the contrary, combined magnetization and <sup>57</sup>Fe Mössbauer spectroscopy,<sup>7</sup> polarized neutron,<sup>8</sup> <sup>145</sup>Nd Mössbauer spectroscopy,<sup>9</sup> and x-ray resonant magnetic scattering studies<sup>10</sup> conclude that the arrangement between Nd and Fe magnetic moments can be considerably noncollinear, although there is no general consensus about the precise mag-

netic structure. In order to obtain a deeper insight into this point, we performed a temperature dependent hard x-ray magnetic circular dichroism (XMCD) study at the Fe  $K$  edge and Nd  $L_{2,3}$  edges.<sup>11</sup> Because of the characteristic element and shell selectivities of XMCD, we were able to experimentally demonstrate the strong noncollinearity between Nd and Fe moments below the SRT. However, the mentioned edges probe the Fe  $4p$  and Nd  $5d$  states, while the main contribution to the magnetic moments comes from the Fe  $3d$  and Nd  $4f$  states. Therefore, in order to finally determine the precise magnetic structure in the low-temperature phase, a parallel XMCD study in the soft x-ray range should be necessary. This study should allow one to quantify the temperature behavior of the Fe and Nd magnetic moments and tilting angles. To this end, we have performed a temperature dependent XMCD study at the Fe  $L_{2,3}$  ( $2p \rightarrow 3d$  transitions) and at the Nd  $M_{4,5}$  ( $3d \rightarrow 4f$  transitions) edges on a Nd<sub>2</sub>Fe<sub>14</sub>B single crystal.

The Nd<sub>2</sub>Fe<sub>14</sub>B crystal has the [001] direction perpendicular to a polished face of 5 × 5 mm<sup>2</sup>. Magnetization measurements were carried out to characterize both the SRT and the coercive field of the specimen (less than 0.4 T at 4.2 K) XMCD measurements at the Fe  $L_{2,3}$  and at the Nd  $M_{4,5}$  edges were performed as a function of temperature in total electron yield detection mode on the Dragon beam line (ID12B) at ESRF.<sup>12</sup> The crystal, positioned in the ultrahigh vacuum chamber, was cleaved *in situ* with the  $c$  axis parallel to the light propagation direction. XMCD signals were obtained as the difference between two x-ray absorption spectra (XAS) recorded consecutively by flipping the magnetic field (of about 1 T) applied along the beam direction. The measured rate of circular polarization is  $P_c = (84 \pm 5)\%$  at the Fe edges and  $P_c = (90 \pm 5)\%$  at the Nd edges.<sup>13</sup> In this geom-

<sup>a)</sup>Electronic mail: luism@posta.unizar.es

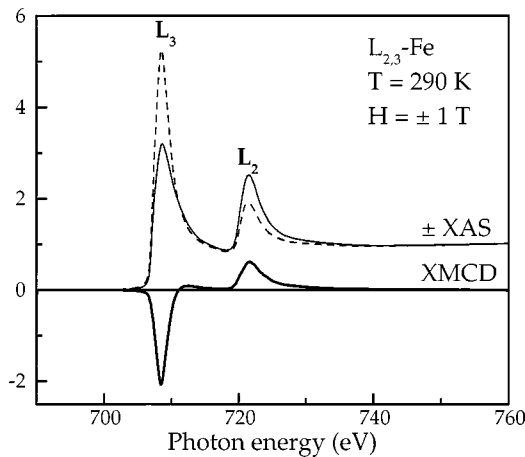


FIG. 1. Normalized  $L_{2,3}$  edge XAS and XMCD spectra of Fe on the  $\text{Nd}_2\text{Fe}_{14}\text{B}$  compound at 290 K.

etry XMCD probes the averages Fe-3*d* and Nd-4*f* magnetic moments projected along the *c* axis.

At each temperature (from 4.2 to 290 K) and absorption edge, several XAS spectra were taken, with parallel and antiparallel relative orientation of the applied magnetic field and the photon helicity. Figures 1 and 2 show a typical example of the normalized averaged XAS and XMCD spectra performed at the Fe  $L_{2,3}$  edges and Nd  $M_{4,5}$  edges, respectively.

In the case of the  $L_{2,3}$  edges of Fe the orbital, spin, and total magnetic moments can be determined by applying the sum rules in the XMCD spectra.<sup>14</sup> As an example, we obtain:  $m_{L,\text{Fe}}=0.10 \mu_B$ ,  $m_{S,\text{Fe}}=2.16 \mu_B$ , and  $m_{\text{Fe}}=2.26 \mu_B$  at 290 K with an absolute error estimated about 10%, while the relative one (versus temperature) is not larger than 3%–4%. The obtained total magnetic moment agrees satisfactorily with the values determined by other techniques.<sup>3</sup> The determined orbital magnetic moment is in agreement with the  $\leq 0.1 \mu_B$  suggested from the strong anisotropy observed in the Fe hyperfine field<sup>15</sup> and larger than the  $0.06(3) \mu_B$  predicted by band structure calculations.<sup>16</sup> The orbital to spin magnetic moments ratio ( $m_L/m_S=0.046$ ) is also in good

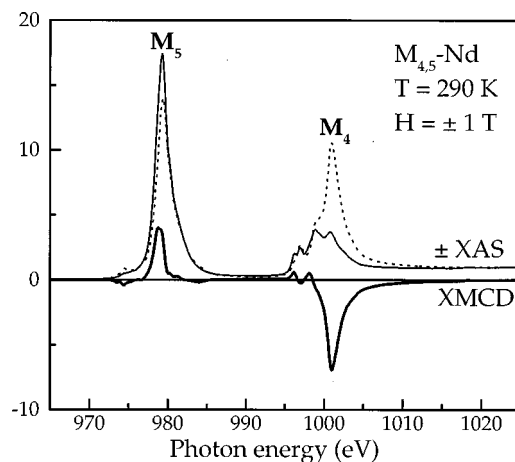


FIG. 2. Normalized  $M_{4,5}$  edge XAS and XMCD spectra of Nd on the  $\text{Nd}_2\text{Fe}_{14}\text{B}$  compound at 290 K.

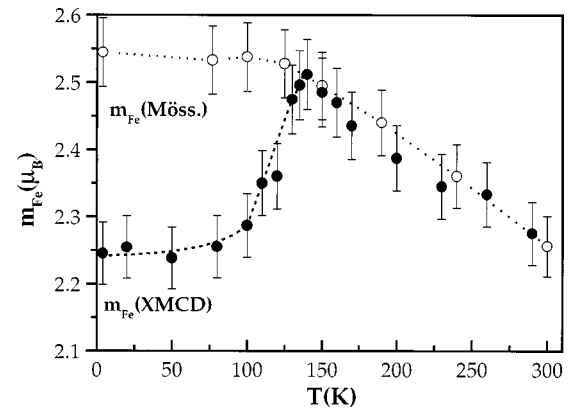


FIG. 3. Temperature dependence of the modulus of Fe magnetic moment obtained from  $^{57}\text{Fe}$  Mössbauer spectroscopy (Ref. 7) and of the projected (along the *c* axis) Fe moment derived from application of sum rules to Fe  $L_{2,3}$ -edge XMCD measurements.

agreement ( $\sim 10\%$ ) with that determined from previous XMCD measurements performed on the same compound at room temperature.<sup>17</sup>

In Fig. 3, the temperature dependence of the iron magnetic moment (per atom), obtained as explained previously, is shown. As the temperature decreases, a linear increase of the magnetic moment is observed, and below 140 K there is a continuous and strong reduction of the magnitude. As XMCD measures the projection of the moment along the *c* axis, this reduction is due to the SRT that  $\text{Nd}_2\text{Fe}_{14}\text{B}$  exhibits at this temperature. Comparing the projection ( $m_{\text{XMCD}}$ ) with the modulus (determined from  $^{57}\text{Fe}$  Mössbauer spectroscopy<sup>7</sup>), it is easy to obtain the temperature dependence of the average Fe tilting angles with respect to the *c* axis,  $\theta_{\text{Fe}}(T)$ , as shown in Fig. 4. The  $\theta_{\text{Fe}}(T)$  set obtained with this method agrees satisfactorily, within a discrepancy of about 5%, with the tilting angles determined from Mössbauer measurements.<sup>7</sup>

It should be desirable to apply the above-explained procedure to the neodymium moments, because the possible noncollinearity of these moments with respect to the iron ones was the origin of the tremendous controversy that ap-

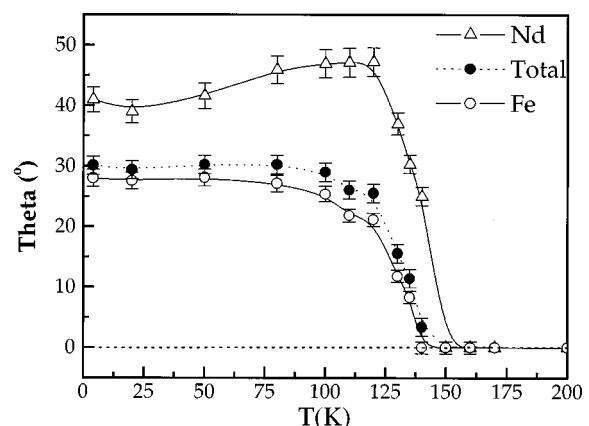


FIG. 4. Temperature dependence of the angles formed between the *c* axis and the average Fe sublattice magnetization, the average Nd sublattice magnetization, and the total magnetization of the  $\text{Nd}_2\text{Fe}_{14}\text{B}$  compound.

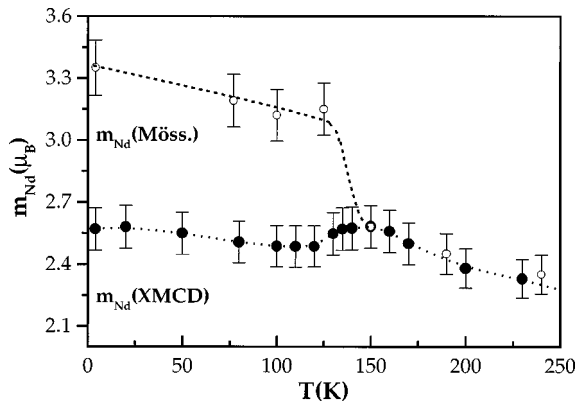


FIG. 5. Temperature dependence of the modulus of Nd magnetic moment obtained from combined magnetization and  $^{57}\text{Fe}$  Mössbauer spectroscopy (Ref. 7) and of the projected (along the  $c$  axis) Nd moment derived from XMCD measurements at the Nd  $M_{4,5}$  edge. The latter data are scaled to the former ones at the high temperature phase.

peared in the literature, and Mössbauer spectroscopy<sup>7,9</sup> results do not arrive at a unique solution. Application of sum rules at the Nd  $M_{4,5}$  edges is not so straightforward as in the Fe ones, because due to the intermixing between core split edges, the spin moment is strongly overvalued. Anyway we have applied the sum rules to the Nd  $M_{4,5}$  edges to assure that there are no effects in the temperature dependence of the neodymium orbital to spin ratio. With this result, the magnetic moment of the Nd atom is proportional to  $(I^+ - I^-)/(I^+ + I^-)$ , where  $I^+$  ( $I^-$ ) is the experimental intensity detected with parallel (antiparallel) orientation between the magnetic field and the photon helicity. Hence, we can obtain a temperature dependence of the Nd magnetic moment that can be scaled (in the high temperature phase) to the absolute values obtained from Mössbauer spectroscopy.<sup>7</sup> In Fig. 5, we compare the temperature dependence of the modulus of the Nd magnetic moment obtained from Ref. 7 (with the well-known jump at the SRT) with the evolution of the projection along the  $c$  axis of the Nd magnetic moment. In the high temperature phase the match of the scaled signals is remarkable, while in the low- $T$  phase the SRT induces a clear discrepancy. From the observed difference, it is obvious to determine the temperature dependence of the average Nd tilting angles with respect to the  $c$  axis,  $\theta_{\text{Nd}}(T)$ , that are shown in Fig. 4.

In Fig. 4, we present both  $\theta_{\text{Fe}}(T)$ ,  $\theta_{\text{Nd}}(T)$  and the total  $\theta(T)$ , where  $\theta$  is the angle between total magnetization and the  $c$  axis. The angle,  $\theta$ , has been calculated by the vectorial addition of the determined moments of Nd and Fe. This microscopically determined  $\theta(T)$  is in good agreement ( $\sim 4\% - 5\%$ ) with the values determined from magnetization measurements<sup>3-5</sup> which gives validity to the method used in this work. There are three interesting results to stress from Fig. 4.

(a) There is a clear delay in the reorientation of the Fe sublattice with respect to that of the Nd sublattice by  $\sim 10$  K. This is evidence of a shift in temperature between both sublattice magnetization. Other techniques have had great difficulty in uncoupling the Fe and Nd contributions.

(b) A strong noncollinearity between Fe and Nd moments is evidenced at all temperatures below the SRT. This result is in agreement with previous experiments,<sup>7-11</sup> but also represents a precise determination of the dynamics of each magnetic sublattice in the low temperature phase. The behavior of the Nd moments is even more complex than expected: by cooling  $\theta_{\text{Nd}}$  increases up to  $47^\circ$  at 110 K, but later on it decreases to  $41^\circ$  at 4.2 K.

(c) Theoretical crystal electric field models<sup>3,5</sup> do not predict this strong noncollinear behavior. Therefore typical approximations usually performed in theoretical models to overcome the difficulties that these complex magnetic systems present must be revised.

This work was supported by Spanish DGICYT Project No. MAT96-0448. We gratefully acknowledge H. Maruyama for useful discussions, M. Sagawa for providing the single crystal, and the help of N. B. Brookes and K. Larsson during the experimental work at the ESRF (Proposal HE-143).

- <sup>1</sup>M. Sagawa, S. Fujimura, N. Togawa, H. Yamamoto, and Y. Matsuura, *J. Appl. Phys.* **55**, 2083 (1984).
- <sup>2</sup>J. J. Croat, J. F. Herbst, R. W. Lee, and F. E. Pinkerton, *Appl. Phys. Lett.* **44**, 148 (1984).
- <sup>3</sup>J. F. Herbst, *Rev. Mod. Phys.* **63**, 819 (1991), and references therein.
- <sup>4</sup>D. Givord, K. S. Li, and R. Perrier de la Bathie, *Solid State Commun.* **51**, 857 (1984).
- <sup>5</sup>K. Tokuhara, Y. Ohtsu, F. Ono, O. Yamada, M. Sagawa, and Y. Matsuura, *Solid State Commun.* **56**, 333 (1985).
- <sup>6</sup>J. Cadogan, J. P. Gavigan, D. Givord, and H. S. Li, *J. Phys. F: Met. Phys.* **18**, 779 (1988).
- <sup>7</sup>H. Onoedera, A. Fujita, H. Yamamoto, M. Sagawa, and S. Hirose, *J. Magn. Magn. Mater.* **68**, 6 (1987); **68**, 15 (1987).
- <sup>8</sup>D. Givord, K. S. Li, and F. Tasset, *J. Appl. Phys.* **57**, 4100 (1985); quoted by D. Givord, K. S. Li, J. M. Moreau, and P. Tenaud, *J. Magn. Magn. Mater.* **54-57**, 445 (1986).
- <sup>9</sup>I. Nowik, K. Muraleedharan, G. Wortmann, B. Perscheid, G. Kaindl, and N. C. Koon, *Solid State Commun.* **76**, 967 (1990).
- <sup>10</sup>A. Koizumi, K. Namikawa, H. Maruyama, K. Mori, and H. Yamazaki, *Jpn. J. Appl. Phys., Part 1* **32**, 332 (1993).
- <sup>11</sup>J. Chaboy, L. M. García, F. Bartolomé, A. Marcelli, G. Cibin, H. Maruyama, S. Pizzim, A. Rogalev, J. Goedkoop, and J. Goulon, *Phys. Rev. B* **57**, 8424 (1998).
- <sup>12</sup>J. Goulon, N. B. Brookes, C. Gauthier, J. Goedkoop, C. Goulon-Ginet, M. Hagelstein, and A. Rogalev, *Physica B* **208**, 199 (1995).
- <sup>13</sup>M. Drescher, G. Snell, U. Kleineberg, H. J. Stock, N. Müller, U. Heinzmann, and N. B. Brookes, *Rev. Sci. Instrum.* **68**, 1939 (1997).
- <sup>14</sup>B. T. Thole *et al.*, *Phys. Rev. Lett.* **68**, 1943 (1992); P. Carra *et al.*, *ibid.* **70**, 694 (1993).
- <sup>15</sup>R. Fruchart *et al.*, *J. Phys. F: Met. Phys.* **17**, 483 (1987).
- <sup>16</sup>B. Szpunar, W. E. Wallace, and J. Szpunar, *Phys. Rev. B* **36**, 3782 (1987).
- <sup>17</sup>S. Imada, T. Muro, S. Suga, K. Kobayashi, H. Maruyama, and H. Yamazaki, *J. Electron Spectrosc. Relat. Phenom.* **78**, 279 (1996).